PHYSICAL REVIEW A VOLUME 44, NUMBER 4 15 AUGUST 1991

ARTICLES

Ergodic properties of high-dimensional symplectic maps

M. Falcioni
Dipartimento di Fisica, Università "La Sapienza," piazzale Aldo Moro 2, 00185 Roma, Italy

U. Marini Bettolo Marconi
Dipartimento di Matematica e Fisica, Università di Camerino, via Madonna della Carceri, 62032 Camerino, Italy

A. Vulpiani
Dipartimento di Fisica, Università de l'Aquila, via Vetoio, 67010 Coppito-l'Aquila, Italy
(Received 15 March 1991)

We report extensive numerical studies on the long-time behavior of a high-dimensional system of coupled symplectic maps as a function of their number N and of the nearest-neighbor coupling strength ϵ. The system, at a fixed value of ϵ, displays regular motion only in a small fraction of the phase space, whose volume vanishes exponentially with N. Regarding the chaotic motion, we find a scaling behavior of the mean-square fluctuation σ of the maximal Lyapunov exponent about its average value over initial conditions: $\sigma \simeq (1/N)^{\alpha}$ where $\alpha = O(\sqrt{\epsilon})$. Nevertheless, also for large systems, one observes a very weak Arnold diffusion, and different trajectories, with a high value of the Lyapunov exponents, maintain some of their own features for a very long time. Finally, we study the localization properties of the tangent vector. For chaotic trajectories, at small values of ϵ, an initially small perturbation increases only in a few directions; due to the translational invariance of the system, this behavior may be seen as a failure of ergodicity and also as a confirmation of the relevance of the Nekhoroshev scenario in high-dimensional systems.

I. INTRODUCTION

A great deal is known about Hamiltonian systems and symplectic maps at low dimensionality [1]. In the case of Hamiltonians with two degrees of freedom, the Kolmogorov-Arnold-Moser (KAM) tori have dimension 2 and separate different regions of the three-dimensional surface of constant energy. This fact allows the coexistence of disjoint regions characterized by different behaviors: in other words, there exist regular and chaotic regions with various degrees of chaoticity. This situation is illustrated in oval billiards [2] where, for specific values of the parameters, up to eight disjoined chaotic regions coexist, each with its own maximal Lyapunov exponent (MLE).

When the number of degrees of freedom exceeds three (or two in the case of maps), the KAM tori cease to separate the phase space and one can observe, instead, the phenomenon known as Arnold diffusion [3]. The existence of such a diffusion has been proved in a variety of cases. It is common wisdom that the Arnold diffusion is a generic property of Hamiltonian systems. However, it is not completely clear how effectively it works as the number of degrees of freedom, N, varies; e.g., it is not clear if this diffusion can be responsible, at large N values, for the quick filling of phase space that would assure the approach to a canonical ensemble within nonastronomical time. Some examples of Hamiltonian systems with $N=3$ are known in which Arnold diffusion exists, but is very slow [4]. In fact, there exist classes of initial conditions that originate chaotic trajectories whose long-time behaviors, as far as they have been determined numerically, show different statistical properties, i.e., different MLE and correlation functions [4].

It is known that a generic Hamiltonian system is neither completely regular nor completely chaotic [5]; however, it is not a simple task to determine such features, in particular in high-dimensional systems. In the present paper we study the above problem in a system of symplectic maps with many degrees of freedom. The study of symplectic maps rather than of Hamiltonian systems is motivated by the major simplicity from the computational point of view, because it avoids the problems of the integration algorithm. Moreover, since N symplectic maps can be thought as a Poincaré map of a Hamiltonian system with $N+1$ degrees of freedom, one expects that many features of symplectic maps also hold in Hamiltonian systems. We consider a system of symplectic coupled maps of the form

$$\begin{aligned} \underline{\theta}(n+1) &= \underline{\theta}(n) + \underline{I}(n) \pmod{2\pi} , \\ \underline{I}(n+1) &= \underline{I}(n) + \epsilon \underline{\nabla} F[\underline{\theta}(n+1)] \pmod{2\pi} , \end{aligned} \tag{1}$$

where $\underline{\theta}$ (the angles), $\underline{I}$ (the actions), and $\underline{\nabla} = (\partial/\partial\theta_1, \ldots, \partial/\partial\theta_N)$ are N-dimensional vectors; n is the discrete time evolution index.

One can easily convince oneself that the time a trajectory needs to visit a D-dimensional space must grow at least exponentially with D. Let us divide the space into cells of linear size ϵ and call τ the typical time needed to reach a neighboring cell. Since the number of cells scales as ϵ^{-D}, the time to visit all of them following a random walk is

$$\mathcal{T} \simeq \tau \epsilon^{-2D} \simeq \exp(\text{const} \times D) .$$

In the case of a chaotic motion with some correlation, the above estimate can be taken as giving, at least, the right order of magnitude. So, to study the asymptotic behavior of the system, we follow its evolution for a time, T, that is finite but large with respect to some suitably defined characteristic time, and then extrapolate the results at $T\to\infty$. Since the time necessary to visit a D-dimensional space is so large, this seems to us the only viable approach.

In Sec. II we shall introduce the model and discuss the statistics of the MLE, λ, on varying the initial conditions as a function of ϵ and N. One observes that the probability of finding a regular zone (i.e., $\lambda\simeq 0$) decreases exponentially with N. However, although at large N almost all the trajectories show a chaotic behavior, they maintain different values for the MLE. Practically at fixed ϵ and N we observe that the histogram of λ, obtained following many trajectories starting from different initial conditions, has a finite variance σ. As $N\to\infty$ we have $\sigma\to 0$, i.e., the system reaches a unique chaotic phase; nevertheless, one observes that for small ϵ this trend is very slow. The most probable value of the MLE, that is, the λ where the histogram attains its maximum, is close to the λ obtained with a random-matrices approximation. In Sec. III we discuss the localization properties of the tangent vectors, showing how these features can give nontrivial indication on the ergodicity of the system. In Sec. IV the reader may find some final remarks and a discussion of the numerical results.

II. THE DISTRIBUTION OF THE MAXIMAL LYAPUNOV EXPONENTS

Let us consider the following system of coupled maps:

$$\begin{aligned}\theta_i(n+1)&=\theta_i(n)+I_i(n) \pmod{2\pi}\ ,\\ I_i(n+1)&=I_i(n)+\epsilon\nabla_i F(\underline{\theta}(n+1)) \pmod{2\pi}\ ,\end{aligned} \tag{2}$$

where $i=1,2,\ldots,N$; we consider periodic boundary conditions: $\theta_{N+1}=\theta_1$, $I_{N+1}=I_1$, and nearest-neighbour coupling:

$$F(\underline{\theta})=\sum_{i=1}^{N}\cos(\theta_{i+1}-\theta_i)\ . \tag{3}$$

The system represented by Eq. (2) is symplectic because its evolution law is given by the canonical transformation whose generator $\mathcal{S}$ is

$$\mathcal{S}(\underline{\theta}',\underline{I})=\sum_{i=1}^{N}\theta_i' I_i-\tfrac{1}{2}\sum_{i-1}^{N} I_i^2+\epsilon F(\underline{\theta}')\ ,$$

through the relations

$$\theta_i=\frac{\partial\mathcal{S}}{\partial I_i},\quad I_i'=\frac{\partial\mathcal{S}}{\partial\theta_i'}$$

if $\underline{\theta}=\underline{\theta}(n)$, $\underline{I}=\underline{I}(n)$, $\underline{\theta}'=\underline{\theta}(n+1)$, and $\underline{I}'=\underline{I}(n+1)$. One can interpret the variables θ_i and I_i as canonical coordinates that describe the evolution at discrete time intervals of a Hamiltonian system. Moreover one can see the map (2) as the Poincaré section of a Hamiltonian system with $N+1$ degrees of freedom. When the coupling constant ϵ vanishes, the system is integrable, and $\epsilon F(\underline{\theta})$ plays the role of the nonintegrable perturbation of the Hamiltonian.

Some insight on the chaotic properties of a trajectory can be obtained by considering the MLE [6], λ, for which we have to introduce the evolution law for the tangent vectors:

$$\begin{aligned}\delta\theta_i(n+1)&=\delta\theta_i(n)+\delta I_i(n)\\ \delta I_i(n+1)&=\delta I_i(n)+\epsilon\{\cos[\theta_i(n+1)-\theta_{i+1}(n+1)][\delta\theta_{i+1}(n+1)-\delta\theta_i(n+1)]\\ &\quad+\cos[\theta_i(n+1)-\theta_{i-1}(n+1)][\delta\theta_{i-1}(n+1)-\delta\theta_i(n+1)]\}\ .\end{aligned} \tag{4}$$

We perform the statistics of the MLE, at fixed ϵ and N, following $\mathcal{N}\gg 1$ trajectories with randomly chosen initial values of the θ_i in the interval $(0,2\pi)$ and initial values of I_i in the interval $(-\pi,\pi)$. For each trajectory we compute the quantity

$$\lambda(T)=\frac{1}{2T}\ln\sum_{i=1}^{N}\frac{[\delta\theta_i^2(T)+\delta I_i^2(T)]}{\sum_{i=1}^{N}[\delta\theta_i^2(0)+\delta I_i^2(0)]} \tag{5}$$

and produce a λ histogram. The maximum integration time T, i.e., the number of iterations applied to the evolution equations, varies with ϵ and was chosen to be $\simeq 10^4$ times the characteristic time of the system, defined as the inverse of λ_p: the maximal Lyapunov exponent extracted from the position of the peak of the histogram.

For $\epsilon=0$ the system is completely regular and consequently $\lambda\equiv 0$ for any initial condition. The numerical computations show that for $\epsilon\neq 0$ the probability of finding regular zones, i.e., the fraction of $\lambda\simeq 0$, decreases exponentially as N grows. In Fig. 1 we show the behavior of P_0, the fraction of the MLE such that $\lambda<=0.002$, as N varies, for the two cases $\epsilon=0.025$ and $\epsilon=0.050$. We find

$$P_0\simeq\exp(-\gamma N) \tag{6}$$

and γ increases with ϵ; in the cases of Fig. 1, one has $\gamma(\epsilon=0.025)\simeq 0.05$ and $\gamma(\epsilon=0.05)\simeq 0.15$. The above values of γ turn out to be rather robust with respect to variations of the cutoff value of λ.

This kind of exponential decay has been observed also

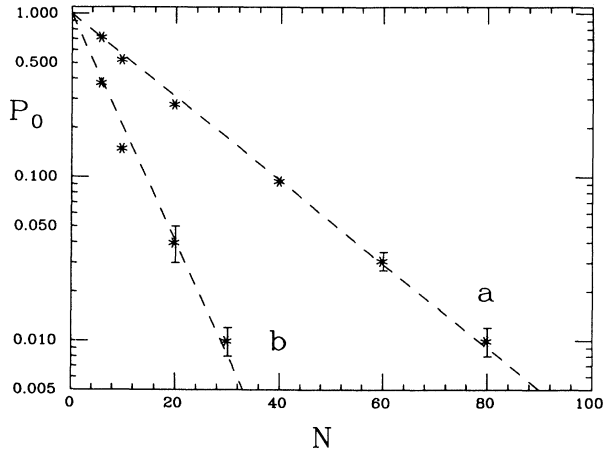

FIG. 1. The fraction of maximal Lyapunov exponents smaller than 0.002 as a function of N for (a) $\epsilon=0.025$ and (b) $\epsilon=0.050$. $T=10^5$ and $\mathcal{N}=500$.

in systems with two coupling constants [7], i.e., an array of two-dimensional maps that have nonzero probability to display chaotic motion, even in the absence of interaction among them. In the present case, it is not possible to repeat the simple argument introduced for the explanation of the above systems, nevertheless it is not difficult to give a heuristic explanation of the result (6). The primary resonances of system (2), with the coupling (3), occur when

$$I_{i+1}(0)-I_i(0)\simeq 0 \quad \text{or} \quad I_{i+1}(0)-I_i(0)\simeq \pm\pi \; ; \tag{7}$$

in order to have a regular motion one has to avoid the resonance condition (7), for $i=1,2,\ldots,N$. If we take all the $I_i(0)$ uniformally distributed in the interval $(-\pi,\pi)$, the probability to have no resonance is $(1-\gamma)^N\simeq e^{-\gamma N}$, if γ is the probability to have a single resonance.

The above result [i.e., Eq. (6)] seems to be in agreement with the common wisdom that Hamiltonian (or symplectic) systems with a large number of degrees of freedom are generically chaotic. However, the analysis of the histogram of the MLE as a function of N and ϵ reveals a nontrivial scenario. The typical behavior of the histogram of λ, at a fixed value of ϵ, is shown in the sequence of Fig. 2, where one can see how ρ, the density of probability of the λ, changes with N. As N increases, the regular zones (with $\lambda\simeq 0$) disappear and the position of the peak of the histogram reaches an asymptotic value. The value of the most probable MLE (obtained from the posi-

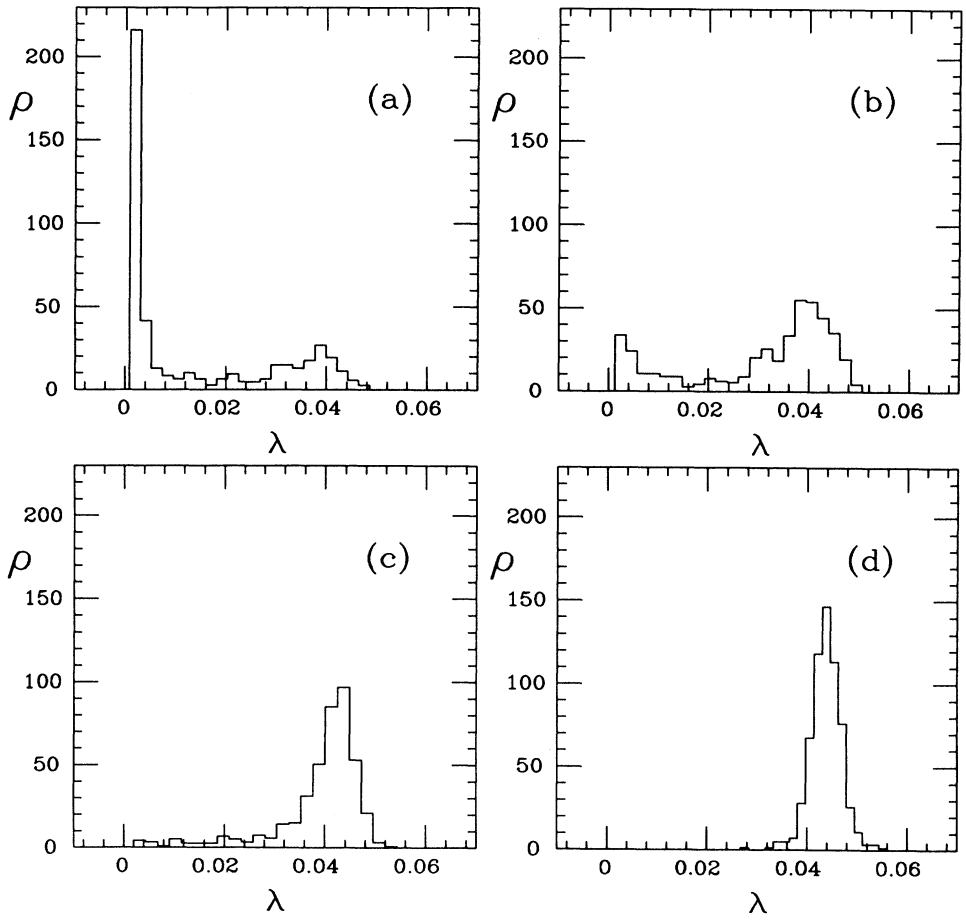

FIG. 2. Probability density of the maximal Lyapunov exponents for $\epsilon=0.025$ and (a) $N=10$, (b) $N=40$, (c) $N=80$, and (d) $N=200$. $T=10^5$ and $\mathcal{N}=500$.

tion of the peak of the histogram) for $N \gg 1$ is well fitted by

$$\lambda_p(\epsilon,N)=\lambda_{as}(\epsilon)+\frac{a}{N} \quad (a<0) . \tag{8}$$

The probability of finding $\lambda \neq \lambda_p$ at fixed ϵ goes to zero as the number of oscillators increases. However the systems with ϵ and N fixed do not appear to approach a unique ergodic phase, at least on the present scales of observation times. In Fig. 3 we show the typical relative fluctuation, as a function of $1/T$, of the λ about $\langle\lambda\rangle \simeq \lambda_p$, i.e., $\sigma=(\langle\lambda^2-\langle\lambda\rangle^2\rangle)^{1/2}/\langle\lambda\rangle$. We fitted the above behavior with the law

$$\sigma(\epsilon,N,T)=\sigma_{as}(\epsilon,N)+\frac{b}{T} \quad (b>0) . \tag{9}$$

The results of the extrapolations, σ_{as} as a function of N, are reported in Fig. 4 for different values of ϵ. All the data are well fitted by

$$\sigma_{as}(\epsilon,N) \simeq (1/N)^{\alpha(\epsilon)} . \tag{10}$$

From Fig. 5, which shows α vs ϵ, one gets some evidence for the following scaling relation:

$$\alpha \propto \sqrt{\epsilon} . \tag{11}$$

The above results show that, for a fixed ϵ, if N is large enough practically all the trajectories are chaotic, but there is no evidence for a unique chaotic region: at least for those times satisfying our criterion of largeness, the trajectories preserve some memory of the initial conditions.

We want to stress that this behavior cannot be explained in terms of perturbative methods in the limit of quasi-integrability, i.e., when the chaotic regions have very small probability. On the contrary, in our case almost all the trajectories have a positive MLE, even if the values of the MLE depend on the initial conditions. Moreover, let us observe that in spite of this apparent

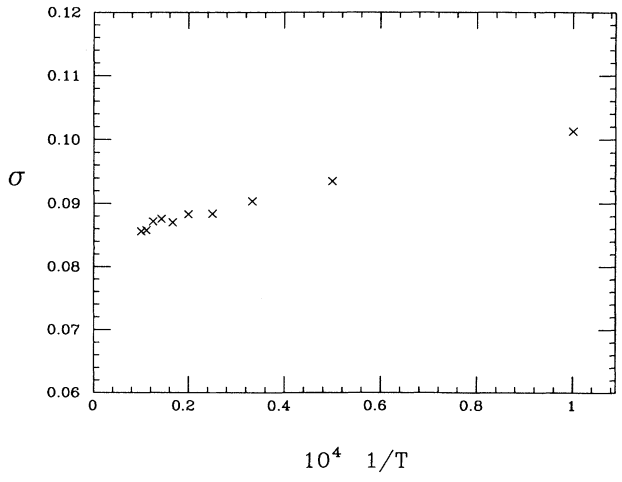

FIG. 3. Relative mean fluctuation of the maximal Lyapunov exponents around their mean value, as function of $1/T$, for $\epsilon=0.050$ and $N=80$. $\mathcal{N}=500$.

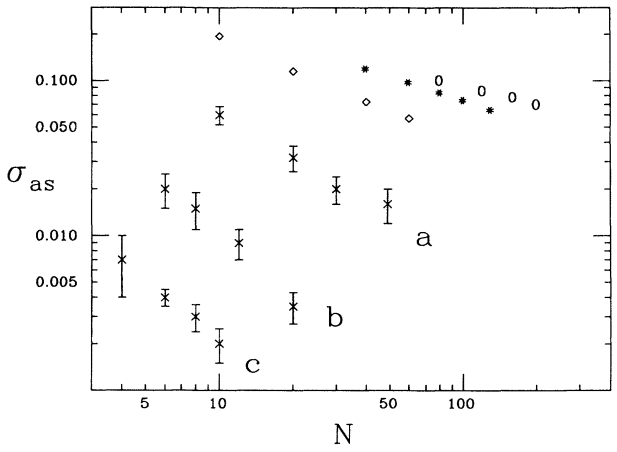

FIG. 4. σ_{as} as function of N for $\epsilon=0.025$ (circles), $\epsilon=0.050$ (stars), and $\epsilon=0.100$ (diamonds). (a) $\epsilon=0.180$, (b) $\epsilon=0.300$, and (c) $\epsilon=0.650$.

"nonergodicity" the most probable value of the MLE is close to the MLE obtained by making use of the so-called random matrices approximations [8]. In this approximation the variables $(\delta\underline{\theta}(n),\delta\underline{I}(n))$ evolve according to Eq. (4) by assigning to each $\theta_i(n)$ random values, uniformly distributed in the interval $[0,2\pi]$ and independently chosen at each step. In Fig. 6 we display the asymptotic value λ_{as} of $\lambda_p(\epsilon,N)$ for $N \to \infty$, versus ϵ together with the MLE that is obtained, for each ϵ, with the random matrices approximation that gives $\lambda \propto \epsilon^{2/3}$ [8].

This shows clearly that while the trajectories have to be considered very chaotic, nevertheless they maintain some of their own peculiarities (e.g., different values of the MLE). From Fig. 4 and Eq. (8) one sees that at a fixed value of ϵ a single chaotic phase is reached as N increases. However, for small values of the coupling constant ϵ the tendency to a unique chaotic phase is very slow.

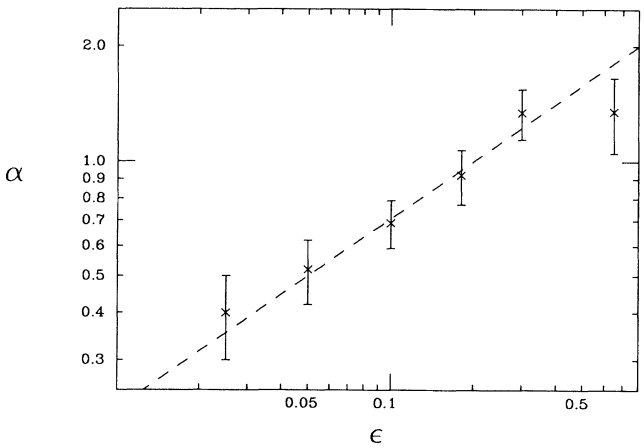

FIG. 5. α vs ϵ; the slope of the dashed line is $\frac{1}{2}$.

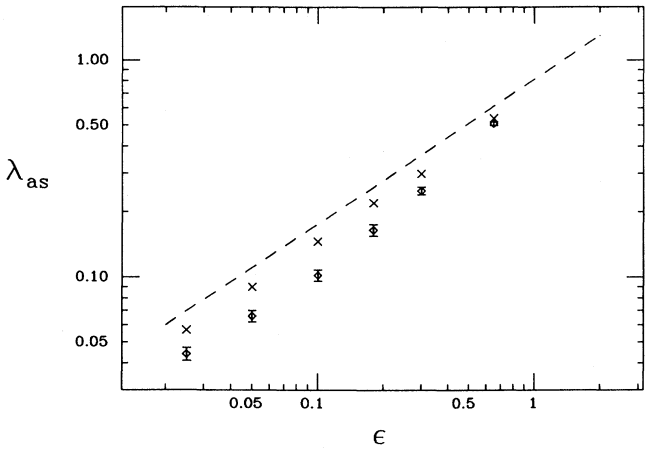

FIG. 6. λ_{as} (diamonds) vs ϵ; the cross symbols are obtained by using the random matrices approximation. The slope of the dashed line is $\frac{2}{3}$.

III. LOCALIZATION PROPERTIES IN THE TANGENT SPACE

In this section we discuss the localization properties of the tangent vector $(\delta\underline{\theta}(n),\delta\underline{I}(n))$. The spatial structure of the tangent vector may be relevant for understanding some features of dynamical systems. See, for instance, Ref. [9] for an application to a cascade model of three-dimensional turbulence. Let us introduce the following auxiliary quantities:

$$z_i^2(n)=[\delta\theta_i(n)^2+\delta I_i(n)^2]/c(n)\ ,$$
$$c(n)=\sum_{i=1}^{N}[\delta\theta_i(n)^2+\delta I_i(n)^2]\ , \tag{12}$$

and

$$\overline{z_i^2}(n)=\frac{1}{n}\sum_{k=1}^{n} z_i^2(k)\ . \tag{13}$$

We have chosen the normalization

$$\sum_{i=1}^{N} z_i^2(n)=\sum_{i=1}^{N}\overline{z_i^2}(n)=1$$

since we are now interested in the "spatial" structure of z_i^2 and $\overline{z_i^2}$ (i.e., their dependence on i). A possible way to characterize the instantaneous and the average localization properties is by defining the following entropylike functions:

$$H_I(n)=-\sum_{i=1}^{N} z_i^2(n)\ln z_i^2(n)\ ,$$
$$H_A(n)=-\sum_{i=1}^{N}\overline{z_i^2}(n)\ln\overline{z_i^2}(n)\ , \tag{14}$$

Similar quantities have been previously introduced in the study of the equipartition problem in chains of nonlinear oscillators, with the aim of getting information on the spreading of the energy among the modes [10], and in other problems (quantum chaos [11]). Let us introduce

$$N_{\rm eff}^{(I)}(n)=\exp[H_I(n)]\ ,$$
$$N_{\rm eff}(n)=\exp[H_A(n)]\ , \tag{15}$$

whose meaning is well evident: $N_{\rm eff}(n)$ is the number of maps "really chaotic," i.e., those that give substantial contribution to the tangent vector $(\delta\underline{\theta},\delta\underline{I})$.

Mainly we observe three different kinds of behavior: (a) at small values of ϵ, for the trajectories with $\lambda\simeq 0$ one has $H_I\simeq H_A\simeq\ln N$, i.e., there is a delocalization in the tangent space; (b) at small values of ϵ, for the chaotic trajectories one has $H_I\simeq H_A\ll\ln N$, i.e., one has both instantaneous and average localization; (c) at large values of ϵ, one has $H_I\ll\ln N$ but $H_A\simeq\ln N$, i.e., there is an instantaneous localization with an average delocalization. Examples of these behaviors are shown in Fig. 7 and 8.

The features of $z_i^2(n)$ [and of $H_I(n)$] can be understood following the argument put forward in Ref. [12]. Practically one can show that $(\delta\theta_i(n),\delta I_i(n))$ obeys an equation very similar to a stationary Schrödinger equation on

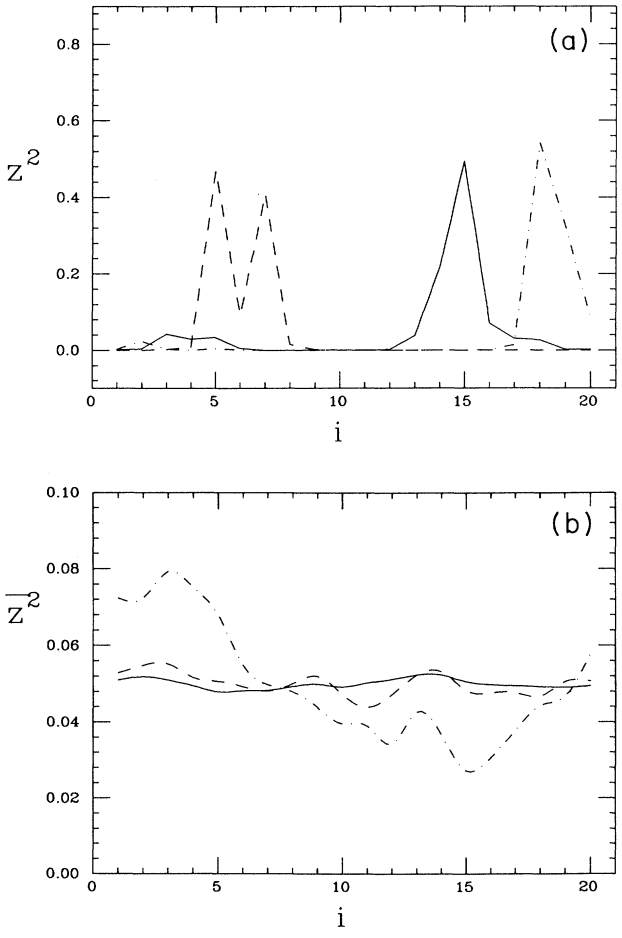

FIG. 7. (a) $z_i^2(n)$ vs i for $N=20$ and $\epsilon=0.3$: $n=3000$ (solid line), $n=5000$ (dashed line), and $n=7000$ (dot-dashed line). (b) $\overline{z_i^2}(n)$ vs i for $N=20$ and $\epsilon=0.3$: $n=10^4$ (dot-dashed line), $n=10^5$ (dashed line), and $n=10^6$ (solid line).

a two-dimensional lattice [13], in a potential given by the dynamics of the system (2). The instantaneous localization (delocalization) is the sign of the localization (delocalization) of the wave function in the random (periodic) potential that one obtains when the dynamics is chaotic (regular). For the chaotic motions the instantaneous localization does not seem to correspond to some relevant feature.

On the contrary the average localization can be viewed as the signal in the tangent space that ergodicity is broken. We use here "broken ergodicity" in the sense of Ref. [14]. Indeed, let us note that in the absence of broken ergodicity, because of the translational invariance of the model, one expects that

$$\overline{z_i^2}(n) \simeq \frac{1}{N} ,$$

i.e., $N_{\text{eff}}(n) \simeq N$ for very large value of n. For small value of ϵ we observe $N_{\text{eff}}(n) \ll N$, i.e., the chaotic motion, in some sense, is localized on a small fraction of the maps. Some similar features of localization in the tangent space have been observed in other systems too [15]. However, in such systems there is no translational invariance, therefore the localization cannot be interpreted, as in our case, as a signature of a broken ergodicity. We want to stress that also in a system of coupled rotators [16], with continuous time, some phenomena of chaos localized on few rotators have been observed.

Let us observe that when case (b) takes place we have also that

$$\overline{\cos(\theta_{i+1} - \theta_i)} \neq 0 \tag{16}$$

for some of the i for which the time equation (7) holds. Nevertheless, the position of such resonances [i.e., the i such that Eq. (7) and (16) hold] does not seem in correspondence with the position of the peaks of the $\overline{z_i^2}$.

Unfortunately at fixed value of ϵ, N_{eff} depends on the initial conditions, so that it is difficult to give an estimation of its behavior as a function of ϵ.

IV. DISCUSSION AND REMARKS ON THE NUMERICAL RESULTS

In this section we shall discuss in some detail the numerical results that were reported in the preceding sections.

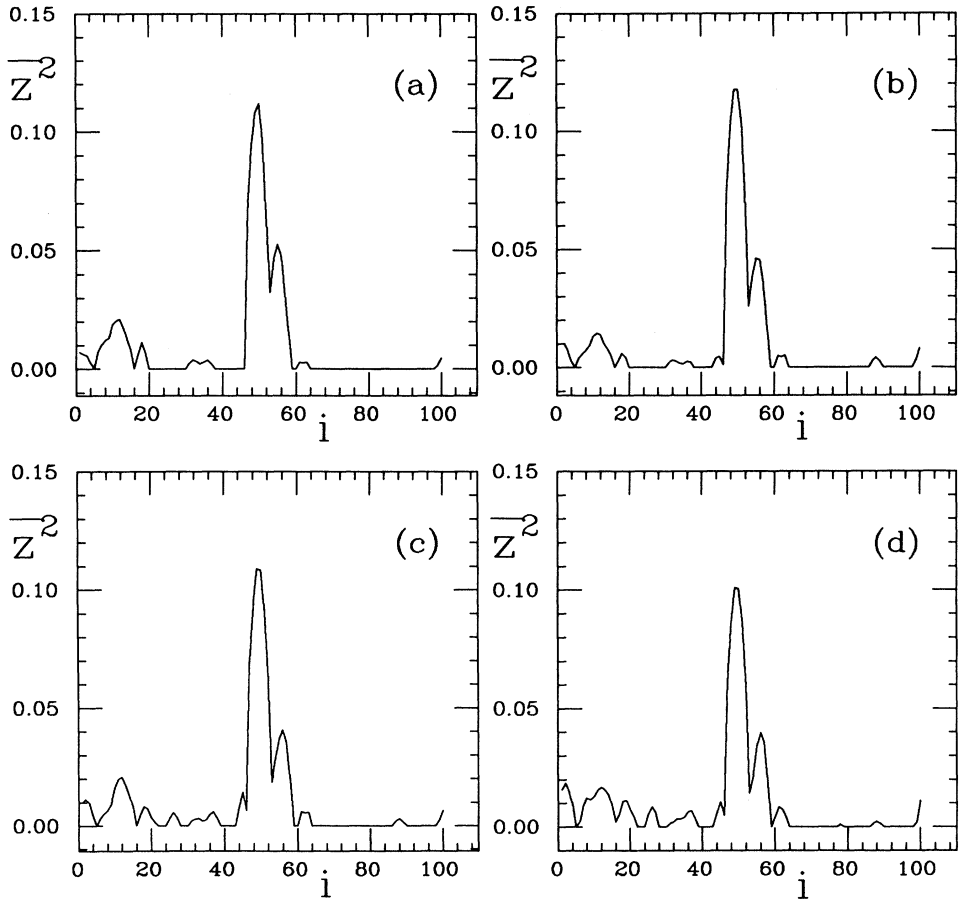

FIG. 8. $\overline{z^2}_i(n)$ vs i for $N=100$ and $\epsilon=0.05$: (a) $n=0.5\times10^6$, (b) $n=1.0\times10^6$, (c) $n=1.5\times10^6$, and (d) $n=2.0\times10^6$.

First of all we stress that the nontrivial dependence of the MLE on the initial conditions is a property completely different from the fluctuations in time of the effective Lyapunov exponent, computed along a trajectory. The latter aspect of the question, for high-dimensional symplectic maps, has been studied in Ref. [17]. In Fig. 9 we show the time behavior of the MLE, computed for different initial conditions, for times very much larger than those used to get the histograms. One can see that after a time $O(10^5)$ up to the time 2×10^6, the differences due to the different initial conditions are much larger than the fluctuations along each trajectory. This is a clear indication that, in very large systems too, the Arnold diffusion could be very slow, and that the histograms of Sec. II are realistic representation of the situation for much larger times. Let us note that, while the most probable value of the MLE of a large system ($N=100-500$) with a small ϵ is in reasonable agreement with the random matrices approximation, the same system seems almost nonchaotic with respect to other properties. For instance, there are some indications that each trajectory needs a very long time to "forget" its initial condition and to invade a reasonable part of the phase space. In Fig. 10, which shows N_{eff} vs n up to $n=2\times10^6$, for different initial conditions, one may observe a tendency to saturation or a very slow growth.

Another way to put in evidence this very slow relaxation may be obtained by the examination of a quantity related to the overlap with the initial conditions. This approach follows the spin-glass theory [18]. A possible function measuring the overlap between the state at time n and the state at time 0 is the following:

$$C(n)=\frac{1}{\Delta}\sum_{k=(n-\Delta)}^{n}\left[\frac{1}{N}\sum_{i=1}^{N}f(I_i(k)-I_i(0))\right], \tag{17}$$

where $f(x)$ is a periodic function decreasing in the interval $[0,\pi/2]$, $f(0)=1$, and $f(\pi/2+x)=-f(\pi/2-x)$. When $I_i(n)=I_i(0)$ (e.g., for $\epsilon=0$), that is to say $I_i(n)$ and

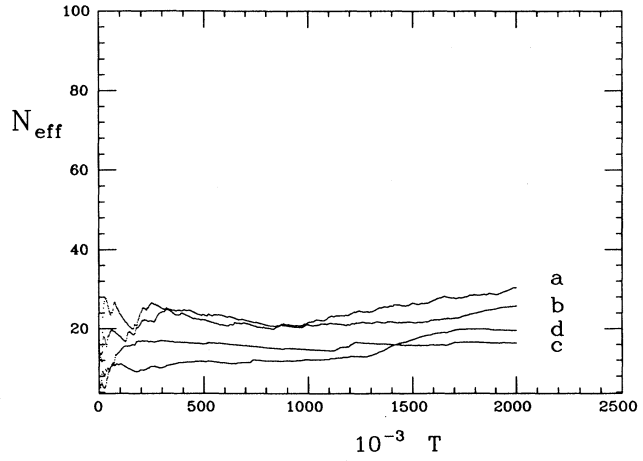

FIG. 10. N_{eff} vs T for $N=100$ and $\epsilon=0.05$, with different initial conditions. The initial conditions are the same as in Fig. 9.

$I_i(0)$ are exactly overlapping, one has $C(n)=1$. On the contrary, if $I_i(n)$ and $I_i(0)$ are completely uncorrelated, one has $C(n)=0$. The time average on an interval Δ around n has been introduced in order to smooth the short-time fluctuations. In the computations shown here we have used $f(x)=\cos(x)$ and $\Delta=10^3$; however, the results do not depend very much on the details of $f(x)$ and the value of Δ. One expects that (apart from small fluctuations) $C(n)$ is a decreasing function of n; an estimate of the time that is necessary for a good exploration of the phase space may be given by the characteristic time n^* such that $C(n^*)\simeq0$.

In Fig. 11 we show $C(n)$ vs n for different initial conditions, in the case $\epsilon=0.05$. The very slow decreasing of $C(n)$ is well evident and it is very difficult to give an estimate of n^*; a tentative rough extrapolation would give $n^*\geq O(10^7)$. Note that the typical time given by the MLE, i.e., $t_\lambda\simeq1/\lambda_p$, is $O(10)$, which is $\ll n^*$.

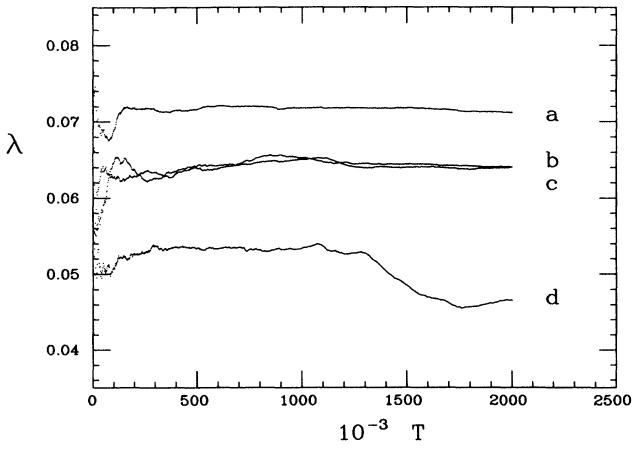

FIG. 9. λ vs T for $N=100$ and $\epsilon=0.05$, with different initial conditions. Figure 8 corresponds to curve *a*.

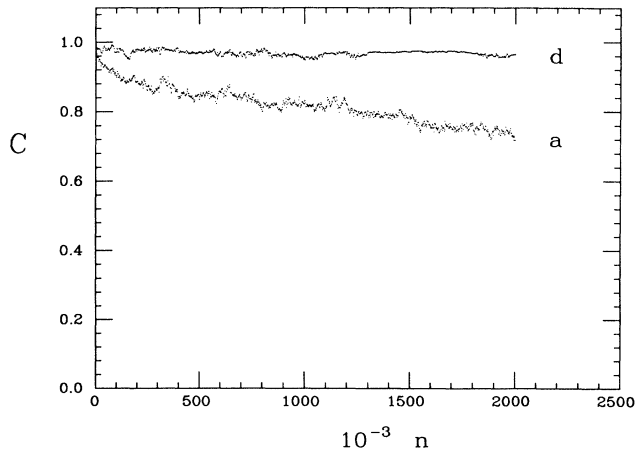

FIG. 11. C vs n for $N=100$ and $\epsilon=0.05$, with different initial conditions.

The existence, at low values of the coupling constant, of characteristic times much larger than t_λ has been stressed also in the study of diffusion properties of system (2), (3), without the periodicity condition on the actions [19], confirming the relevance of the Nekhoroshev scenario [20] also in high-dimensional systems with a non-negligible coupling constant [21].

ACKNOWLEDGMENTS

We thank M. Feingold, K. Kaneko, and S. Ruffo for useful discussions. One of us (A.V.) is grateful to the Institute for the Scientific Interchage of Torino for the invitation to the workshop "Complexity and Evolution," where part of this paper was completed.

[1] A. J. Lichtenberg and M. A. Lieberman, *Regular and Stochastic Motion* (Springer-Verlag, Berlin, 1983).
[2] G. Benettin and J. M. Strelcyn, Phys. Rev. A **17**, 773 (1978).
[3] V. I. Arnold and A. Avez, *Ergodic Problems of Classical Mechanics* (Benjamin, New York, 1968).
[4] G. Contopoulos, L. Galgani, and A. Giorgilli, Phys. Rev. A **18**, 1183 (1978); M. Pettini and A. Vulpiani, Phys. Lett. A **106**, 207 (1984); P. Magnenat, Cel. Mech. **35**, 329 (1985); K. Kaneko and R. J. Bagley, Phys. Lett. A **110**, 435 (1985); A. Malagoli, G. Paladin, and A. Vulpiani, Phys. Rev. A **34**, 1550 (1986).
[5] F. Vivaldi, Rev. Mod. Phys. **56**, 737 (1984).
[6] G. Benettin, L. Galgani, A. Giorgilli, and J. M. Strelcyn, Meccanica **15**, 9 (1980); **15**, 21 (1980).
[7] G. Gyorgyi, F. A. Ling, and G. Schmidt, Phys. Rev. A **40**, 5311 (1989).
[8] G.Parisi and A. Vulpiani, J. Phys. A **19**, L425 (1986); G. Paladin and A. Vulpiani, *ibid.* **19**, 1881 (1986); R. Livi, A. Politi, S. Ruffo, and A. Vulpiani, J. Stat. Phys. **46**, 147 (1987).
[9] M. H. Jensen, G. Paladin, and A. Vulpiani, Phys. Rev. A **43**, 798 (1991).
[10] R. Livi, M. Pettini, S. Ruffo, M. Sparpaglione, and A. Vulpiani, Phys. Rev. A **31**, 1039 (1985).
[11] M. Feingold, D. M. Leitner, and O. Piro, Phys. Rev. A **39**, 6507 (1987); G. Casati, L. Molinari, and F. Izrailev, Phys. Rev. Lett. **64**, 1851 (1990).
[12] R. Livi and S. Ruffo, in *Nonlinear Dynamics,* edited by G. Turchetti (World Scientific, Singapore, 1989), p. 220.
[13] J. L. Pichard and G. Sarma, J. Phys. C **14**, L617 (1981).
[14] R. G. Palmer, Adv. Phys. **31**, 669 (1982).
[15] K. Kaneko, Physica **23D**, 436 (1986).
[16] G. Benettin, L. Galgani, and A. Giorgilli, Nuovo Cimento B **89**, 103 (1985).
[17] H. Kantz and P. Grassberger, Phys. Lett. A **123**, 437 (1987); A. Crisanti, G. Paladin, and A. Vulpiani, J. Stat. Phys. **53**, 583 (1988).
[18] M. Mezard, G. Parisi, and M. A. Virasoro, *Spin Glass Theory and Beyond* (World Scientific, Singapore, 1987).
[19] K. Kaneko and T. Konishi, Phys. Rev. A **40**, 6130 (1989); T. Konishi, Progr. Theor. Phys. (Suppl.) **98**, 19 (1989); T. Konishi and K. Kaneko, J. Phys. A **23**, L715 (1990).
[20] N. N. Nekhoroshev, Usp. Mat. Nauk **32**, 5 (1977).
[21] M. Casartelli, Nuovo Cimento B **76**, 97 (1983); M. Pettini and M. Landolfi, Phys. Rev. A **41**, 768 (1990).